IOPscience iopscience.iop.org

Home Search Collections Journals About Contact us My IOPscience

A quantitative evaluation of the dynamic cathodoluminescence contrast of gliding dislocations in semiconductor crystals

This article has been downloaded from IOPscience. Please scroll down to see the full text article.

2004 J. Phys.: Condens. Matter 16 S269

(http://iopscience.iop.org/0953-8984/16/2/032)

View the table of contents for this issue, or go to the journal homepage for more

Download details:
IP Address: 129.252.86.83
The article was downloaded on 28/05/2010 at 07:45

Please note that terms and conditions apply.

Institute of Physics Publishing Journal of Physics: Condensed Matter

J. Phys.: Condens. Matter **16** (2004) S269–S277 PII: S0953-8984(04)66936-0

A quantitative evaluation of the dynamic cathodoluminescence contrast of gliding dislocations in semiconductor crystals

S Vasnyov, J Schreiber and L Hoering

Fachbereich Physik, Martin-Luther-Universitaet Halle-Wittenberg, Friedemann-Bach-Platz 6, D-06108 Halle (Saale), Germany

Received 31 July 2003
Published 22 December 2003
Online at stacks.iop.org/JPhysCM/16/S269 (DOI: 10.1088/0953-8984/16/2/032)

Abstract

Dark cathodoluminescence (CL) defect contrasts observed in CL video movies taken on GaAs and ZnO samples disclose the intrinsic recombination properties of glide dislocations during their slip motion. This way, the kinematical SEM CL microscopy provides, for the first time, direct information on the possible relationship between the dynamics and electronic activity of glide dislocations as expected from structural alterations or kink processes related to defect movement. The dark CL defect contrasts observed for various dislocation types in both materials indicate defect-bound non-radiative excess carrier recombination. Quantitative CL contrast analysis is performed to discover differences in the recombination strength of distinct dislocation structures resulting from the type and dynamic state of the glide dislocations studied.

1. Introduction

Glide dislocations in semiconductor crystals are expected to exhibit intrinsic electrical and optical properties determined by electronic states originating in the dislocation core structure and/or the local strain field [1][1]. In many cases dislocations are recognized as very efficient excess carrier recombination centres. The scheme in figure 1 illustrates the relationship between the defect structure and recombination activity. In particular, the polar character of the dislocation core structure as expected in compound semiconductor crystals is considered (see footnote 1).

Dislocation recombination activity may be revealed by SEM CL microscopy [2]. CL contrast measurements yield quantitative values of the CL contrast of single dislocations, which can be analysed to deduce the defect recombination strength defined by

$$C_{\mathrm{CL}} = \lambda \cdot C',$$

[1] The Huenfeld convention [8] is used in the following to term mobile edge type dislocations supposing a glide set slip mechanism.

 © 2004 IOP Publishing Ltd Printed in the UK

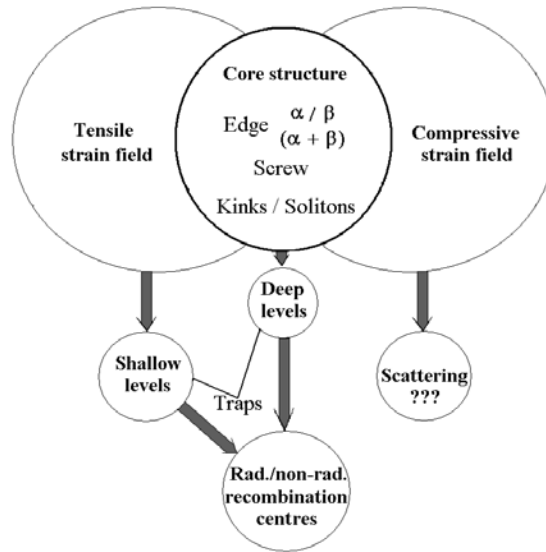

Figure 1. A scheme of a possible relationship of a dislocation structure comprising core and strain field to defect recombination activity.

where λ is the total defect strength, C' is a CL contrast profile factor and C_{CL} stands for the experimentally measured CL contrast value. The quantity λ represents the specific recombination property of a dislocation and describes the recombination flux for a given local excess carrier density. According to the CL contrast theory developed for dislocations [3], λ figures as the linear recombination velocity and is determined by the defect parameters as

$$\lambda = \pi r_D^2/\tau_D,$$

where r_D and τ_D are the defect radius and defect-induced carrier lifetime, respectively. Consequently, defect recombination strengths depend on the density and distribution of electronic states related to the structure of dislocations.

Kink sites corresponding to the slip motion of a dislocation are believed to be excess carrier recombination centres localized in the core region of dislocations [4]. Namely, the density of kinks changes with the glide velocity or curvature of the defect line. Steady velocity of a dislocation segment is given by the product of the kink line density N_L, the kink's diffusion velocity ν_k and distance h between the Peierls potential valleys [5]:

$$\nu = N_L \nu_k h.$$

Thus, assuming the kink sites act as effective recombination centres, one may expect a clear correlation between the CL contrast strength and the dislocation velocity due to the formal proportionality between the kink density and the defect recombination strength:

$$\lambda \sim N_L.$$

Kinematical SEM CL imaging is a unique tool to disclose the recombination properties of dislocations during their slip motion [6]. CL video movies offer direct access to the dynamics and electronic activity of gliding dislocations related to kink processes or other structural alterations on small dislocation segments [7].

The contrast behaviour of gliding single dislocations can be studied by analysing the quantitative CL data gained from each frame of the SEM CL image sequences. A so-called

dynamic contrast diagram (DCD) is created which provides simultaneously information on both dislocation dynamics and recombination activity reflected by momentary local CL contrast behaviour.

In the present paper kinematical CL microscopy is applied to study the dynamic CL contrast behaviour of edge- and screw-type dislocation segments in GaAs and ZnO. In both materials the dislocations appear as CL dark contrasts indicating non-radiative recombination activity. The dislocations are shown to propagate in a strain gradient by thermal activation and/or move due to an REDG (radiation enhanced dislocation glide) effect [4] caused by the electron beam probe used for the SEM CL imaging procedure.

2. Experimental details

Kinematical SEM CL experiments were carried out using a conventional SEM apparatus (JSM 6400, Jeol) equipped with a CL attachment (Mono CL, Oxford Instruments) and cooling stage (CF302, Oxford Instruments). Sequential CL imaging, recording panchromatic signals with frame rates up to 10 fps, was performed utilizing an electronic system developed for real time image acquisition and fast data processing (Digital Image Scanning System (DISS 4), Fa. Point Electronic GmbH), which, in particular, provides high capacity quantitative data storage as well.

For the purpose of local plastic deformation under *in situ* conditions a special microindentation set-up was developed and installed. The sample treatment and corresponding CL observation could be carried out at temperatures between 295 and 72 K.

Sample materials studied were III/V and II/VI semiconductor bulk crystals with low-index sample surfaces. The different crystalline samples were chosen for their zincblende lattice (GaAs) and wurtzite structure (ZnO), respectively.

3. Results

3.1. Quantitative analysis of the CL contrast of resting dislocations

In order to quantify defect contrasts as displayed in the CL micrographs, the following convention is commonly used to define the value of the CL contrast [3]:

$$C_{\mathrm{CL}} = (I_{\mathrm{D}} - I_0)/I_0.$$

Here I_{D} and I_0 mean the CL intensity at the dislocation and in the undisturbed matrix, respectively. CL contrast values are usually obtained by means of one-dimensional CL intensity profile measurements.

Figure 2(a) shows a 3D plot of a quantitative CL map representing the CL defect contrast spot of a threading dislocation segment. A lateral decrease of the CL signal in the vicinity of the defect is clearly seen. In figure 2(b) the same local reduction of CL intensity is revealed in side view for a quantitative analysis which provides a CL contrast value of about 0.5.

In our SEM CL experiments on ZnO samples, differences in recombination activity of the polar A(g)- and B(g)-type glide dislocations in a wurtzite lattice [9] have been discovered by performing quantitative CL contrast evaluation. The CL contrast properties of the A(g) and B(g) dislocations were studied at threading dislocation segments formed in the $\langle 11\bar{2}0\rangle$ arms of indentation-induced dislocation rosettes on a $(10\bar{1}0)$ sample surface. The detailed findings are presented in figures 3(a) and (b).

The dark spot-like patterns related to the individual single defect segments are found to have different contrast strengths in the CL picture. The intensity profile extracted along AB

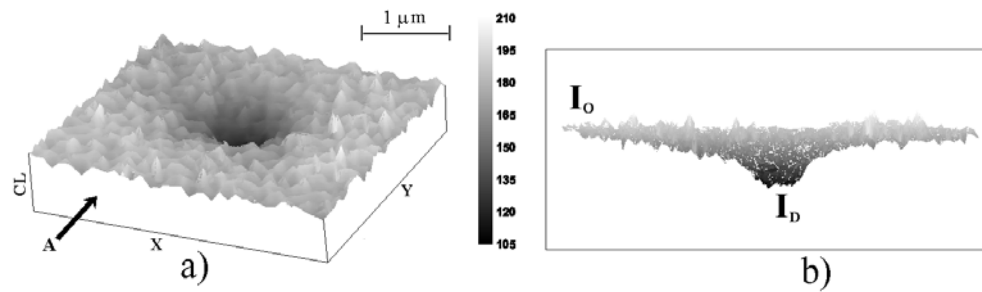

Figure 2. A 3D presentation of a map of CL intensity at threading dislocation segment in a ZnO sample by top view (a) and A-side view (b) showing local defect-related and matrix intensity levels.

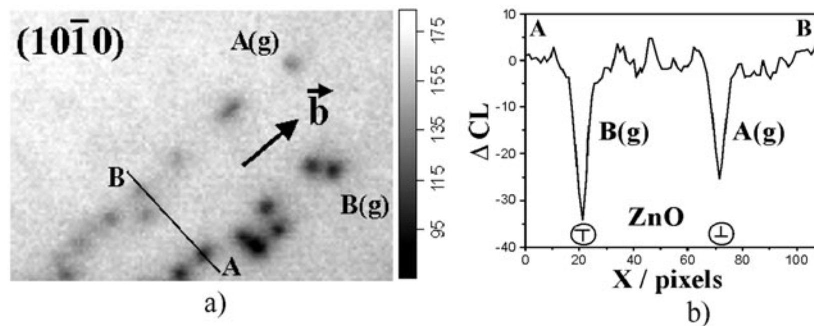

Figure 3. The difference in CL contrasts at A(g)- and B(g)-type glide dislocations in ZnO revealed by CL micrograph (a) and profile measurement (b), respectively, at single threading dislocation segments.

yields the ratio of the CL contrast values for the A(g) and B(g) dislocations concerned:

$$C_{A(g)}/C_{B(g)} = \lambda_{A(g)}/\lambda_{B(g)} = 0.7.$$

The contrast ratio corresponds immediately with the difference in recombination activity [10] of the A(g)- and B(g)-type dislocations. This proved dependence of CL contrast on dislocation type may be ascribed to the opposite polar core structure in the A(g) and B(g) dislocations. Thus, it could be expected that similar CL contrast variations should occur between edge- and screw-type dislocations. This is demonstrated in figures 4 and 5. Figure 4(a) is a CL image containing among others the CL contrast pattern of a part of a dislocation half-loop expanding in a surface-parallel slip plane.

Between s and f (figure 4(a)) along the defect line an edge- and screw-type segment can be distinguished. The change of CL contrast strength is recognized over this individual loop structure by means of a Bezier curve [11] guided local contrast analysis, as illustrated by the scheme given in figure 4(b). A set of CL intensity profiles aa′ crossing the dislocation loop line is taken between the start ‘s’ and the finish ‘f’. Such a measuring procedure provides a number of CL intensity profiles, which are to be analysed to evaluate the local CL contrast values. The edge-type segment is found to show the stronger CL contrast. The derived change of the CL contrast strength from s to f is displayed in figure 5.

The CL contrast values measured on the edge-type dislocation segment are found to be clearly increased in comparison with those at the screw part. Thus, enhanced recombination activity for the edge-type segment can be concluded.

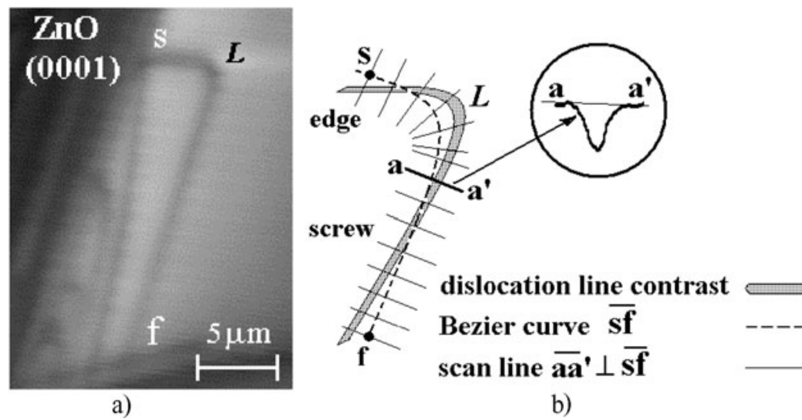

Figure 4. The analysis of CL contrasts at edge- and screw-parts along the dislocation loop structure sf shown in a CL image (a). The procedure of local profile measurement is sketched in (b).

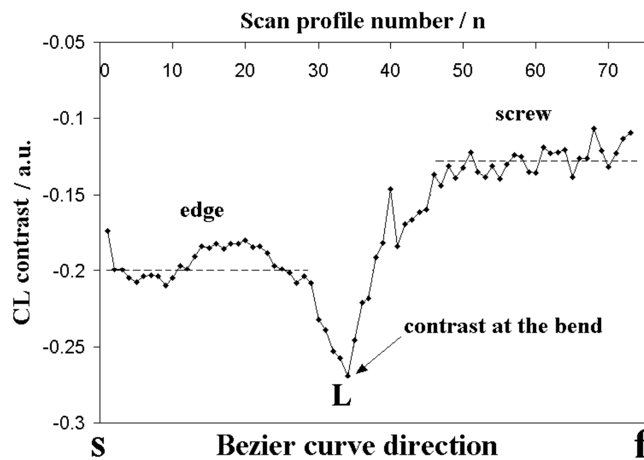

Figure 5. The variation of CL contrast along the dislocation sf. Edge- and screw-type segments are found to exhibit different contrast strengths. Additional enhancement of CL contrast in the bend region L is seen.

At the sharply bent part of the loop line an additional rise of contrast is observed. This phenomenon might be explained by regarding kinks as effective carrier recombination centres. Their density could be increased in the corner region for geometrical reasons [12].

3.2. Quantitative analysis of dynamic CL contrast at moving dislocations

The contrast behaviour of gliding single dislocations can be deduced from the CL video movies recorded utilizing the full dynamic range of CL signals in order to calculate the actual values of CL defect contrasts, which correlate directly with the movement of the dislocation. The determination of the dynamic CL defect contrast values is based on the original CL data gained from each frame of the SEM CL image sequences. For this purpose, CL intensity profiles are generated along an arbitrarily chosen line AB that is fixed in an identical image area for all frames of the entire sequence forming a given movie (figure 6(a)). Distinct positioning of the recording line allows us to register defect-related CL contrasts within any particular dislocation arrangement.

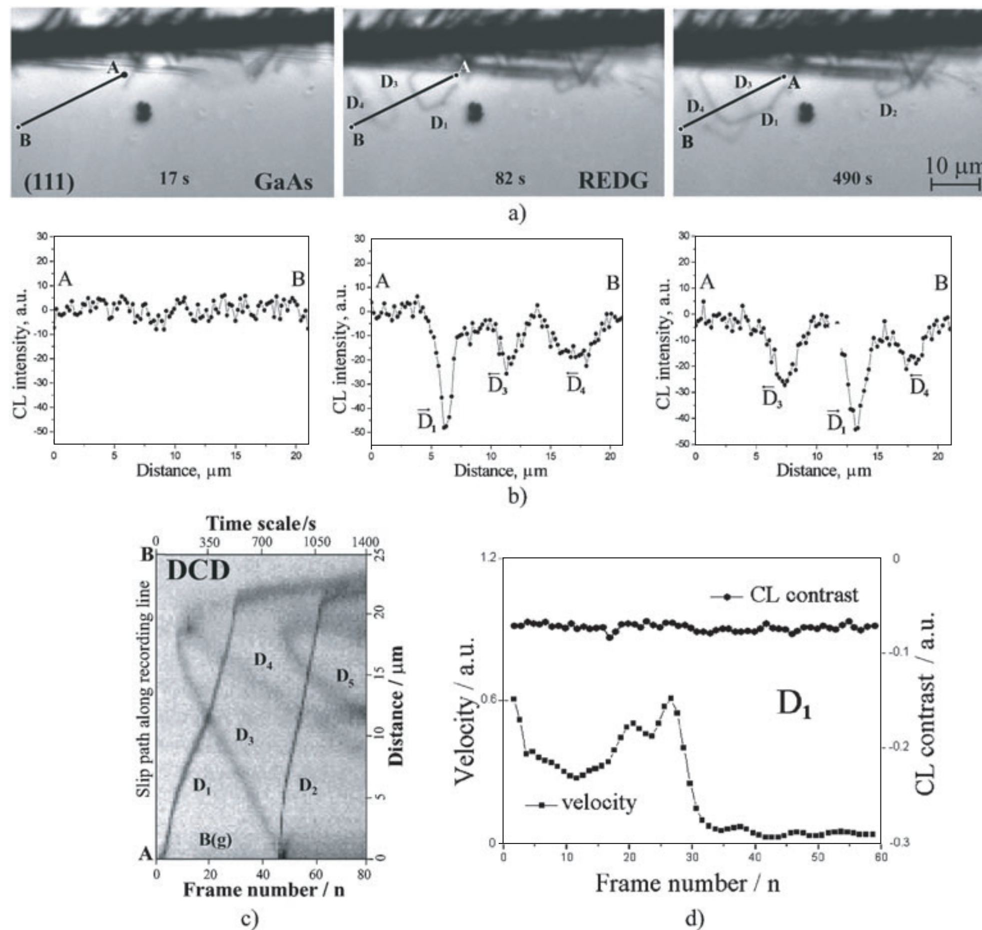

Figure 6. The analysis of the dynamics and correlated CL contrast properties as observed at individual glide dislocations by means of kinematical SEM CL. The sequence of CL images (a) selected from the CL movie shows the propagation of dislocation segments ($D_1, D_2, \ldots$) constituting an expanding half-loop structure. Examples of CL intensity profiles along AB crossing mobile parts of half loops are given in (b). The corresponding DCD plot (c) is a complete set of the CL intensity profiles transformed into grey scale presentation, and put together over the frame number axis which relates to the timescale. This DCD provides data on slip motion and momentary CL contrast behaviour for several dislocation segments. The slip velocity and correlated CL contrast value for the 60°-line segment D_1 during slip and resting state is shown graphically in (d).

To analyse the CL defect contrasts as a function of dislocation slip path or time, the values of CL intensities over the recording line AB are measured identically pixel-by-pixel from A to B in all subsequent frames of the given movie. The resulting CL intensity profiles are finally arranged in a special kind of diagram, the DCD. The DCD represents, at the same time, the frame number, slip path, and momentary value of CL contrast at the dislocation segments crossed by the recording line AB. The local dislocation velocity can be derived from the slope of a DCD pattern.

On the other hand, the DCD displays the progress of a CL intensity profile, measured between points A and B in each frame at the same place, against time.

Quantitative treatment of CL contrast profiles includes preliminary noise filtering and local background correction followed by computation of the values of the CL defect contrasts.

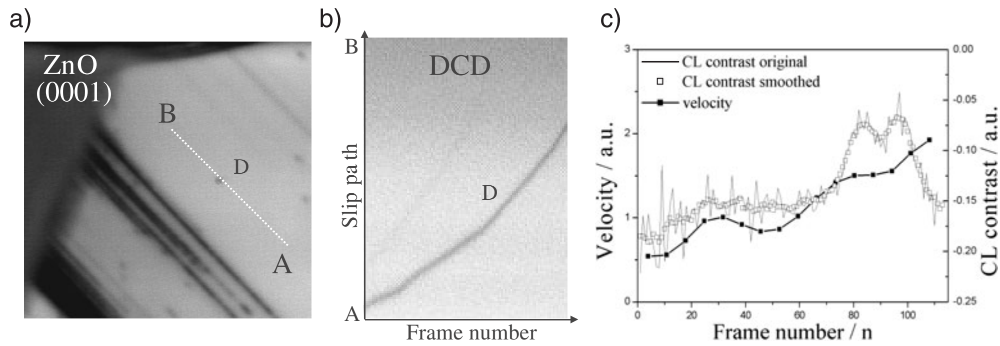

Figure 7. The dynamics and CL contrast behaviour of a threading dislocation segment in ZnO. Figures 7(a) and (b) show a CL micrograph and derived DCD plot, respectively, for a mobile threading dislocation D. Analysis of the DCD yields dynamic contrast values and local velocity, both plotted in figure 7(c).

In particular, specific DCD plots can be created from the same CL movie by analysing several distinct segments along an isolated dislocation line.

The new DCD technique is applied to examine the dynamic CL contrast behaviour of edge- and screw-type dislocation segments in GaAs as demonstrated in figures 6(a)–(d).

Both edge- and screw-type parts appear as dark CL contrasts. The movement of fresh glide dislocations in various $\{111\}\langle 1\bar{1}0\rangle$-type slip systems as observed on the (111) oriented sample is illustrated by the sequence of CL images shown in figure 6(a). The dislocations introduced by *ex situ* scratching propagate in a strain gradient and move under electron beam excitation due to the REDG effect at room temperature [13].

Studying the (111) sample configuration allows for the recognition of isolated individual dislocation half loops expanding in surface-parallel glide planes, so that occurring edge-type ($30°, 60°, 90°$) and screw line parts belonging to same dislocation loop structure can be investigated in detail. In figure 6 complete analysis is performed for a 60°-line segment D_1. Examples of extracted CL intensity profiles and the DCD plot according to the fixed recording line AB are shown in figures 6(b) and (c). The DCD plot represents the dynamics and contrast behaviour of up to five different dislocation segments ($D_1 \ldots D_5$). Defect motion in opposite directions and with different slip velocity is displayed.

Figure 6(d) contains the correlated data of deduced dynamics and CL properties as derived for D_1. From analysis of the corresponding DCD pattern, the slip velocity and contrast values as a function of time are gained in order to recognize any relationship between the behaviour of the glide speed and recombination activity as observed at this dislocation segment. However, in the present case no response of CL contrast to the dynamic state of the defect is revealed.

The results of a similar study of the dynamic CL contrast behaviour at a moving threading dislocation segment in ZnO are presented in figures 7(a)–(c). In the CL picture (a) the slip path A to B of a selected defect D is illustrated.

The DCD plot in figure 7(b) proves accelerated slip of segment D. The derived slip velocity is shown in figure 7(c); it exhibits a varying increase over the time of observation. An apparent link between CL contrast and local speed may be concluded. However, the fact that the contrast decreases as the dislocation velocity increases is not expected.

To get a better understanding of a possible relationship between the defect dynamics and intrinsic recombination activity more detailed considerations of the REDG effect at individual dislocations appears to be rather useful. Such an experiment employing kinematical SEM CL to observe the REDG properties of a single dislocation is dealt with in figures 8(a)–(c).

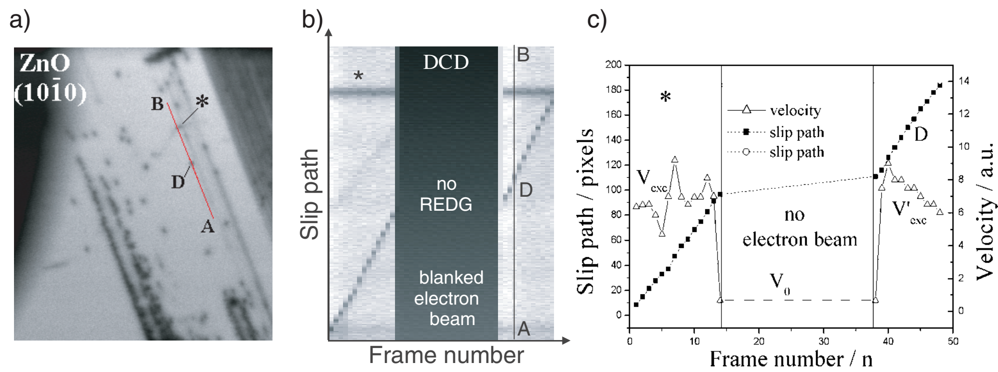

Figure 8. The recognition of the REDG effect for dislocation slip by the $\{10\bar{1}0\}\langle 11\bar{2}0\rangle$ glide system in ZnO. The movement of the threading dislocation segment under conditions with and without electron beam excitation is followed by observing the CL contrast spot D shown in the CL image (a). The corresponding DCD plot is given in (b). Slip velocities determined for REDG phases and the period of pure thermally activated glide are displayed in (c); an enhancement factor of $\sim$12 is obtained.

Figure 8(a) is a frame taken from the entire movie that shows the movement of a threading dislocation spot marked D. The DCD plot in figure 8(b) contains the pattern of the mobile defect D and of a resting defect labelled '$*$'. The dark area in the DCD corresponds to the beam-off state.

Under electron beam excitation, the threading dislocation D has comparable velocity before and after the beam-off period. During the time when the electron beam was blanked, slow dislocation glide remains. Under this condition, dislocation motion is only due to thermal activation and local stress. For the threading dislocation observed here the velocity ratio is found to be

$$V_{\text{exc}}/V_0 = 12.$$

Motion of the dislocation under electron beam irradiation and its essential slowing down in excitation pause while the electron beam is blanked prove a clear REDG effect in the ZnO sample [13] and hint at stimulation of kink processes by the dislocation-bound carrier recombination [14].

4. Conclusions

Scanning CL video movies using kinematical SEM offer straightforward access to the dynamics and intrinsic recombination activity of the dislocations moving through the crystal lattice matrix. In GaAs and ZnO samples chosen for their zincblende and wurtzite lattice structures, respectively, dynamical properties and CL contrast behaviours of individual dislocations are considered in detail.

Advanced analysis of the CL movies provides the so-called DCD, which represents a special plot comprising correlated information on the local velocity and momentary CL contrast value of particular slipping dislocation segments. The DCD plot is utilized to explore a possible relationship between the dislocation dynamics and intrinsic recombination activity.

For the first time, distinct contrast behaviour in the case of dislocation-related non-radiative carrier recombination is recognized in ZnO at the screw- and edge-type dislocations and, in

particular, for the polar A(g) and B(g) edge-type dislocations with opposite core structure. A contrast ratio $C_{A(g)}/C_{B(g)}$ of approximately 0.7 is found at the A(g) and B(g) dislocations; this is in the same range as that measured on screw- and edge-type segments in an identical half-loop structure. At a moving threading dislocation segment of edge-type, an apparent link between the momentary CL contrast value and local speed may be deduced. However, the fact that the contrast decreases as the dislocation velocity increases is not expected.

The results obtained on GaAs show that the dark CL defect contrasts found behave almost independently of the structural type and dynamic state of the glide dislocations studied. Thus, from these experiments kinks cannot be evidenced as the dominating recombination centres.

Acknowledgments

This work was performed in the framework of the 'Graduiertenkolleg 415' der Deutschen Forschungsgemeinschaft.

The authors thank D M Hofmann, Universitaet Giessen, for supplying ZnO samples. Special thanks are given to Dipl.-Eng. Hermann Maehl for technical support.

References

[1] Rebane T Yu and Shreter G Yu *Springer Proc. Phys.* vol 54, ed J H Werner and H D Strunk (Berlin: Springer) p 28
[2] Yacobi B G and Holt D B 1990 *Cathodoluminescence Microscopy of Inorganic Solids* (New York: Plenum) p 125
[3] Schreiber J and Hergert W 1989 *Inst. Phys. Conf. Ser.* **104** 97
[4] Maeda K and Takeuchi S 1996 *Dislocations in Solids* vol 10, ed F R N Nabarro and M S Duesbery (Amsterdam: Elsevier) p 445
[5] Hirth J P and Lothe J 1968 *Theory of Dislocations* (New York: McGraw-Hill)
[6] Hoering L 2001 *Thesis* University of Halle
[7] Hoering L, Schreiber J and Hilpert U 2001 *Solid State Phenom.* **78/79** 143
[8] 1979 *Proc. Int. Symp. Dislocations in Tetrahedrally Coordinated Semiconductors*; *J. Physique Coll.* **40** C6, in the foreword
[9] Osipiyan Yu A and Smirnova I S 1968 *Phys. Status Solidi* **30** 19
[10] Hildebrandt S, Uniewski H, Schreiber J and Leipner H S 1997 *J. Physique* III **7** 1505
[11] Farin G 1983 Algorithms for rational Bezier curves *Comput. Aided Des.* **15** 73–7
[12] Gottschalk H 1983 *J. Physique Coll.* **44** C4 475
[13] Maeda K, Suzuki K, Yamashita Y and Mera Y 2000 *J. Phys.: Condens. Matter* **12** 10079–91
[14] Maeda K and Takeuchi S 1983 *J. Physique Coll.* **44** C4 375